

Research article

urn:lsid:zoobank.org:pub:7132EF90-7CC1-4288-8644-5B9CA0E5A8AC

A new species of snail-eating snakes of the genus *Pareas* Wagler, 1830 (Reptilia: Serpentes) from eastern Himalayas, India

Harshal BHOSALE¹, Pushkar PHANSALKAR², Mandar SAWANT³,
Gaurang GOWANDE⁴, Harshil PATEL⁵ & Zeeshan A. MIRZA^{6,*}

^{1,3}Bombay Natural History Society, Mumbai, Maharashtra 400001, India.

²A/2, Ajinkyanagari, Karvenagar, Pune, Maharashtra 411052, India.

⁴Annasaheb Kulkarni Department of Biodiversity, Abasaheb Garware College, Pune,
Maharashtra 411004, India.

⁴Department of Biotechnology, Fergusson College, Pune, Maharashtra 411004, India.

⁵Department of Biosciences, Veer Narmad South Gujarat University, Surat, Gujarat 395007, India.

⁶National Centre for Biological Sciences, TIFR, Bangalore, Karnataka 560065, India.

*Corresponding author: snakeszeeshan@gmail.com

¹Email: harshabhosale99@gmail.com

²Email: pushkar.phansalkar@gmail.com

³Email: m.sawant@bnhs.org

⁴Email: gaurang.gowande@gmail.com

⁵Email: harshilpatel121@gmail.com

¹urn:lsid:zoobank.org:author:31CD74C9-4433-43D5-8132-1EF39AF0BDC3

²urn:lsid:zoobank.org:author:06BB8F0E-9623-4759-9CBB-44927E43D47A

³urn:lsid:zoobank.org:author:18DE73F8-DB9E-488D-97C1-D5CEC418B160

⁴urn:lsid:zoobank.org:author:1D0ED49C-6286-4E7E-AE14-C0EEB9DBBCAF

⁵urn:lsid:zoobank.org:author:DCDF105B-E163-4C8F-86C7-85C4275974EF

⁶urn:lsid:zoobank.org:author:25F673F0-3FB9-4A4F-81CE-997748CC26E6

Abstract. A new species of snail-eating snakes of the genus *Pareas* Wagler, 1830 is described from the eastern Himalayas. The species *Pareas kaduri* sp. nov. differs from all known species of the genus in bearing the following suite of characters: SVL 455–550 mm, TaL/TL 0.184–0.207, brown dorsum with black transverse bands throughout the body, 15 dorsal scale rows throughout the body and mid-dorsal vertebral scale rows enlarged, 8 rows keeled in males, loreal not touching orbit, ventrals 160–183, subcaudals 65–70 in males, 52 in one female specimen, hemipenis short, unilobed and 6–7 maxillary teeth. Molecular data for mitochondrial 16S rRNA and cytochrome *b* genes further attest the distinctness of the new species, which was recovered as a member of the *Pareas hamptoni* clade. Our work brings the total number of species recognized within the genus *Pareas* to 20.

Keywords. Arunachal Pradesh, biodiversity hotspot, *cyt b*, Indo-Burma, molecular phylogeny, Pareidae, *Pareas kaduri* sp. nov., taxonomy.

Bhosale H., Phansalkar P., Sawant M., Gowande G., Patel H. & Mirza Z.A. 2020. A new species of snail-eating snakes of the genus *Pareas* Wagler, 1830 (Reptilia: Serpentes) from eastern Himalayas, India. *European Journal of Taxonomy* 729: 54–73. <https://doi.org/10.5852/ejt.2020.729.1191>

Introduction

Members of the snake subfamily Pareinae Romer, 1956 are strictly nocturnal, arboreal and are one of the most fascinating groups of snakes that feed on rather unusual prey (Whitaker & Captain 2004; Hosoi *et al.* 2007; Vitt & Caldwell 2014). Members of the subfamily that specialize in feeding on snails present a remarkable case of dietary specialization where they have asymmetry in their dentition on the maxilla to devour prey like snails and slugs (Hosoi *et al.* 2007). Despite their evolutionary significance, these snakes remain poorly studied concerning their habits, habitat and their diversity. The subfamily currently comprises three genera, namely, *Pareas* Wagler, 1830, *Aplopeltura* Duméril, 1853 and *Asthenodipsas* Peters, 1864 (Deepak *et al.* 2018). The genus *Pareas* is the most species-rich among members of the subfamily, with 19 nominate species recognized today (Wallach *et al.* 2014; You *et al.* 2015; Vogel *et al.* 2020), with three species currently recorded from India, i.e., *Pareas andersonii* Boulenger, 1888, *P. monticola* Cantor, 1839 and *P. modestus* Theobald, 1868 (Whitaker & Captain 2004; Lalbiakzuala & Lalremsanga 2019; Vogel *et al.* 2020).

In the course of a herpetological expedition, we surveyed several localities across the northeastern Indian state of Arunachal Pradesh. During the surveys, we collected specimens of *Pareas* which looked visually similar to each other that were later identified to belong to two sympatric species based on the structure of the hemipenis. One population was attributed to the species *P. monticola* based on ventral scale number and lack of keels on dorsal scales and shape of hemipenis. The other, however, could not be attributed to any of the species reported from India, owing to the differences in scalation and hemipenis morphology. To identify the second population that was collected from near Kamlang Wildlife Sanctuary in eastern Arunachal Pradesh, we generated molecular data for the collected specimens and compared them with available museum material. Results from the molecular analysis show that the specimens are genetically distinct from congeners and comparison of morphology of known species further attests the findings. We herein describe the population of *Pareas* from eastern Arunachal Pradesh as a new species following an integrative taxonomic approach incorporating morphological, osteological and molecular data.

Material and methods

Morphology

The study was conducted under permit nos. CWL/Gen/173/2018-19/Pt.V11/2434-43 and CWL/Gen/173/2018-19/Pt.V11/2421-33 issued by the Forest Department of Arunachal Pradesh. Four specimens of the new species were collected in the field by hand, photographed and later euthanized with halothane within 24 hours of capture following ethical guidelines for animal euthanasia (Leary *et al.* 2013). The specimens were fixed in 8% formaldehyde buffer and later stored in 70% ethanol. Liver tissue was collected for molecular work and stored in 95% molecular grade ethanol prior to fixation. The specimens have been deposited in the collection of the Bombay Natural History Society (BNHS), Mumbai, and research collection at the National Centre for Biological Sciences, Bangalore. Measurements were taken with the help of a digital calliper to the nearest 0.1 mm, except SVL and TaL, which were taken with a string and then measured using a scale.

Morphological data for the new species were compared with the type specimens available for examination and other voucher specimens of the congeners and with data from Vogel (2015) and You *et al.* (2015). Dentition asymmetry index was calculated following Hosoi *et al.* (2007).

Abbreviations

CL	=	cephalic length measured from tip of snout to the constriction of the neck
DSR	=	dorsal scale rows, counted at approximately one head length behind the head, midbody, and one head length before vent.
ED	=	eye diameter, widest diameter of the eye
EI	=	eye to labial height measured from the lowest border of the eye to the lower border of the labial
EN	=	eye to nares distance
ES	=	eye to snout length
HL	=	head length measured from snout tip to the angle of the jaw
HW	=	head width measured at the widest part of the head
NW	=	neck width measured at the constriction of the neck
SVL	=	snout to vent length
TaL	=	tail length
TL	=	total length (SVL + TaL)
V	=	ventral scales, counted as directed by Dowling (1951)

Repositories

BNHS	=	Bombay Natural History Society, Mumbai, India
MNHN	=	Muséum national d'histoire naturelle, Paris, France
NCBS	=	Collection Facility of the National Centre for Biological Sciences, Bangalore, India
NHMUK	=	Natural History Museum, London, UK
ZSI	=	Zoological Survey of India, Kolkata, India

Micro-CT scans were generated for the paratype male NCBS BH655 using a Bruker® Skyscan 1272 (Bruker BioSpin Corporation, Billerica, Massachusetts, USA). The head of the specimen was scanned for 210 minutes at a resolution of 5.4 μm and recording data for every 0.4° rotation for 360° with (AL) 1 mm filter. The source voltage for the scan was 65 kV and source current was 153 μA . Volume rendering was performed with CTVOX (Bruker BioSpin Corporation) and images were edited in Adobe Photoshop CS6. Osteological description is based on volume renders retrieved from CTVOX following the terminology of the skull described by Heatwole (2009). Images from CT scans of the new species were compared with existing literature on dentition of *Pareas* spp. (Wang *et al.* 2020) and with CT scan images of museum specimens (Anonymous 2015). Comparative material examined is listed in Appendix 5.

Molecular analysis

Genomic DNA was isolated from the preserved tissues of the holotype and the female paratype and a specimen of *P. monticola* from Kamlang WLS and from near Pakke Tiger Reserve using QIAGEN DNeasy kits following protocols directed by the manufacturer. Molecular methods largely follow Mirza *et al.* (2016) and Mirza & Patel (2018). A fragment of the mitochondrial cytochrome b (*cyt b*) and 16S rRNA were amplified using primers used by Pyron *et al.* (2013) and Mirza *et al.* (2016). A 22.4 μl reaction was set, containing 10 μl of Thermo Scientific DreamTaq PCR Master Mix, 10 μl of molecular grade water, 0.2 μl of each 10 μM primer and 2 μl of template DNA, carried out with an Applied Biosystems ProFlex PCR System. The thermo-cycle profile used for amplification was as follows: 95°C for 3 minutes, (denaturation temperature 95°C for 30 seconds, annealing temperature 48°C for 45 seconds for *cyt b* as well as 16S rRNA, elongation temperature 72°C for 1 minutes) \times 36 cycles, 72°C for 10 minutes, hold at 4°C. PCR product was cleaned using a QIAquick PCR Purification Kit and sequenced with an Applied Biosystems 3730 DNA Analyzer. Sequences of related taxa available from GenBank® were downloaded for molecular phylogenetic reconstruction following taxa sampling as in Wang *et al.* (2020) (Appendix 1),

and the sequences were aligned in MegaX (Kumar *et al.* 2018) using ClustalW (Thompson *et al.* 2002) with default settings. The aligned dataset was subjected to Maximum Likelihood (ML) and Bayesian Inference (BI) on the online portal of W-IQ-TREE at <http://iqtree.cibiv.univie.ac.at/> (Trifinopoulos *et al.* 2016). The model selection for the analysis was set to auto and the analysis was run with an ultrafast bootstrap analysis for 1000 iterations. Non-parametric bootstrap pseudo-replicates were used to assess support of the clades. For the optimal partitioning strategy and evolutionary substitution model, aligned data was analyzed using PartitionFinder ver. 1.1.1 (Lanfear *et al.* 2012), implementing a greedy search algorithm under the Akaike Information Criterion (AIC). Bayesian Inference (BI) was implemented in MrBayes ver. 3.2.2 (Ronquist & Huelsenbeck 2003) and was run for 10 million generations and sampled every 1000 generations. The BI run included five parallel chains, three hot and two cold chains. The standard deviation of split frequencies of the analysis reached were below 0.01, after which the analysis was not continued further. Twenty-five percent of the trees generated were discarded as burn-in. Data were subjected to phylogenetic reconstructions with a generalised time-reversible (GTR) + gamma (G) model as the sequence substitution model, based on the optimal partitioning scheme suggested by PartitionFinder for BI. Un-corrected pairwise p-distance (% sequence divergence) was calculated in MegaX (Kumar *et al.* 2018) with pairwise deletions of missing data and gaps.

Results

Molecular phylogenetics based on 1117 bp of the mitochondrial cytochrome *b* gene revealed that the specimens from eastern Arunachal Pradesh were embedded in a clade containing *P. hamptoni* (Boulenger, 1905), *P. mengziensis* Wang *et al.*, 2020 and *P. formosensis* (Van Denburgh, 1909), and was recovered basal to the entire clade with high support (ML bootstrap 89, BI posterior probability 0.99). Genetic divergence with congeners is 12–24%. Keeled dorsal scales and hemipenis morphology further support the distinctness of the species from other members of the clade and congeners (see below). Molecular phylogeny based on 16S rRNA recovered similar relationships as with *cyt b*.

Class Reptilia Laurenti, 1768
Order Squamata Oppel, 1811
Suborder Serpentes Linnaeus, 1758
Family Pareidae Romer, 1956
Subfamily Pareinae Romer, 1956
Genus *Pareas* Wagler, 1830

Pareas kaduri sp. nov.

urn:lsid:zoobank.org:act:66902402-DD58-4F83-B8B2-381EC46FA395

Figs 1–5, Table 1

Differential diagnosis

A new species of *Pareas* bearing the following suite of characters: (1) SVL 455–550 mm, (2) TaL/TL 0.184–0.207, (3) 15 dorsal scale rows (DSR) throughout body and mid-dorsal vertebral scale rows enlarged, 8 rows keeled in males, (4) loreal not touching orbit, (5) ventrals 160–183, (6) subcaudals 65–70 in males, 52 in one female specimen, (7) hemipenis short, unilobed, (8) 6–7 maxillary teeth, (9) dorsum brown with thin black transverse bands, the head with a large black blotch from which two longitudinal black stripes (3–4 scales wide) run on each side of the neck leaving a pale central portion.

The new species is here compared with congeners based on non-overlapping and differing characters: vertebral scales enlarged (vs not enlarged in *P. chinensis* (Barbour, 1912), *P. macularius* Theobald, 1868, *P. margaritophorus* (Jan 1866), *P. vindumi* Vogel, 2015); loreal not in contact with orbit (vs in contact in *P. boulengeri* (Angel, 1920), *P. monticola* (Cantor, 1839), *P. stanleyi* (Boulenger, 1914), *P. vindumi*) and *Amblycephalus yunnanensis* Vogt, 1922; eight mid-dorsal vertebral scales keeled (all scales smooth

in *P. boulengeri* and *Amblycephalus kuangtungensis* Vogt, 1922, 9–13 keeled dorsal scales in *P. komaii* (Maki, 1931), 3–5 in *P. modestus*); two anterior temporals (vs one in *P. nigriceps* Guo & Deng, 2009); ventrals 160–183 (vs 195–213 in *P. nuchalis* (Boulenger, 1900), 189–194 in *P. iwasakii* (Maki, 1937), 151–160 in *P. stanleyi*, 190–196 in *P. monticola*, 130–160 in *P. margaritophorus*), 6–7 maxillary teeth (vs 4–5 in *P. chinensis* (Barbour, 1912) and *P. boulengeri*, 3–5 in *P. menglaensis* Wang, Che, Liu, Li, Jin, Jiang, Shi & Guo, 2020); prefrontals in contact with orbit (vs not in contact in *P. carinatus* (Boie, 1828)); subcaudals 65–70 in males, 52 in female (vs 71–79 in *P. atayal* You, Poyarkov & Lin, 2015, 37–45 in *P. andersonii*); single nasal (vs two in *P. nuchalis* and *P. stanleyi*); dentition asymmetry index 4.55 in males (13.51 in *P. komaii*, 29.03 in *P. atayal*).

The new species shares several characters with members of its clade and is here compared to each species in greater detail based on differing and non-overlapping characters. The new species differs from *P. formosensis* in bearing keeled dorsal scales (vs smooth in *P. formosensis*), dentition asymmetry index 4.55 in males (vs 16.13 in *P. formosensis*).

The new species differs from *P. mengziensis* Wang, Che, Liu, Li, Jin, Jiang, Shi & Guo, 2020 in bearing 6–7 maxillary teeth (vs 3–5 in *P. mengziensis*) and in having the dorsum with thin black bands (vs connected black reticulations throughout the body in *P. mengziensis*).

The new species is most similar to *P. hamptoni* in sharing the plesiomorphic state, where the loreal shield does not touch the orbit and is separated by the preocular. However, the new species differs from the species as follows: ventrals 160–183 (vs 197–202); two anterior temporals (vs a single temporal scale in *P. hamptoni*); subcaudals 65–70 in males, 52 in female (vs 96 in *P. hamptoni*); bearing 8 keeled dorsal scales (vs only a single row keeled in *P. hamptoni*); hemipenis unilobed and not forked (vs deeply forked in *P. hamptoni*).

Etymology

The specific epithet is a patronym honoring wildlife photographer Sandesh Kadur for his contribution to biodiversity documentation in the Himalayas, in particular Arunachal Pradesh, as well as for his constant support to the authors during the expedition.

Type material

Holotype

INDIA • ♂ adult; Arunachal Pradesh, Lohit District, outskirts of Kamlang Wildlife Sanctuary, found along the road leading to Hawa camp from Parshuram Kund; 27.880711° N, 96.363239° E; 350 m a.s.l. (Datum WGS84); 23 Jul. 2019; Harshal Bhosale, Mandar Savant, Pushkar Phansalkar and Gaurang Gowande leg.; BNHS 3574.

Paratypes

INDIA • 1 ♀; same collection data as for holotype; BNHS 3575 • 2 ♂♂; same collection data as for holotype; 28 Jul. 2019; Zeeshan Mirza, Harshal Bhosale, Mandar Savant, Pushkar Phansalkar and Gaurang Gowande leg.; NCBS BH655–BH656.

Description

Holotype ♂ (BNHS 3574) (Figs 1–4)

The specimen is in good condition, preserved in a coil with its head resting outside the coil (Fig. 2). The specimen bears incisions. The hemipenis is partly everted.

Head short, 15.45 mm comprising 2.22% of total length; high, 6.47 mm, with steeply domed snout in lateral view; upper jaw visible from ventral side. Head distinctly broader (9.3 mm) than neck (4.4 mm).

Snout abruptly tapers, rounded tip in dorsal view (Fig. 3). Rostral subpentagonal, reaching top of the snout; as wide as high with a distinct furrow towards its ventral edge. Upper jaw distinctly longer than lower jaw. Nostrils large, 2.04 long and 1.32 high in the centre, elliptical-shaped, positioned in the centre and posterior half of nasal scale. Paired internasals, wider (2.07 mm) than long (1.26 mm); smaller than prefrontals. Prefrontals slightly wider (2.83 mm) than long (2.59 mm). Frontal hexagonal, 3.87 mm at the widest portion, median length 5.06 mm. Parietals 6.62 mm long, 3.87 mm at its widest anteriorly. Temporals 2+3+3 on both sides, subequal in size, posterior one inserts deeply between supralabial sixth, seventh and eighth. Five nuchal scales, slightly larger than adjacent dorsal scales, bordering parietals. Supraocular larger than preocular; preocular small, subequal. Loreal slightly longer (1.68 mm) than high (1.54 mm). Two postoculars, subequal in size. Eye large, circular, 3.13 mm (eye diameter/head height 0.48) diameter with a spherical pupil. Seven supralabials, seventh longest. First to third supralabials smallest, first supralabial only contacts second supralabial, rostral and nasal. Second supralabial in contact with nasal, preocular, loreal and first and third supralabials. Third supralabial in contact with preocular, second and fourth supralabials and making contact remotely with loreal. Supralabials separated from the orbit by a crescent-shaped subocular.

Mental short, broad, triangular. Infralabials 7, anterior five infralabials short and narrow, fifth onwards larger. First infralabials of both sides in broad contact, separate the mental from the genials. Sixth infralabial broadest. First six infralabials in contact with the genials. Anterior genials almost twice as long as wide; anterior genials in broad contact, posterior genials only in remote contact.



Fig. 1. *Pareas kaduri* sp. nov. Holotype, ♂ (BNHS 3574) in life. Photograph by Zeeshan A. Mirza.

Body laterally compressed, ventral surface a little flattened. Dorsal scales in 15:15:15 rows. Dorsal scales imbricate, regularly arranged, vertebral and adjoined scale rows enlarged and larger than the outermost dorsal scales. Eight scale rows on the mid-dorsum (including vertebral rows) keeled; other dorsal scale rows scales smooth and glossy, lacking apical pits. Ventral scales 160 in number + 2 preventrals. Anal shield undivided, slightly larger than last ventral scale, its posterior margin overlaps nine small, irregular scales on each side, in addition to pair of larger subcaudals medially. Subcaudals paired, 70 in number. Tail terminates in a sharp tapering apical spine. Total length 694 mm, tail length 144 mm, tail/total length ratio 0.207.

Hemipenial morphology (paratype NCBS BH655)

The organ is fully everted and expanded (Fig. 4). Hemipenis short, unilobed, stout and unicaliculate; lobe extends for about 60% of the hemipenis; capitulum restricted to sulcate and dorsal surfaces of the organ, covering nearly half of the lobe's length at the level of the sulcus spermaticus; capitulum smooth, except for two rows of calyces spanning almost the entire width of the organ; on asulcate surface, lobes ornamented with three to four parallel broken rows of mediolaterally enlarged and papillate body calyces; sulcus spermaticus simple; the sides of the sulcus spermaticus are smooth; truncus and hemipenial base is wrinkled and completely nude.

Colouration in preservative (Fig. 2)

Overall, in a shade of brown with 28 paired black transverse bands from nape to the vent. Some of these bands are distinct, whereas some are merely black spots that connect rudimentarily to form bands. The head bears a large black blotch from which two black longitudinal stripes (3–4 scales wide) run on each side of the neck leaving a pale central portion. The ventral scales are white or cream colored with sparse black mottling.

Dentition (paratype, ♂ NCBS BH655) (Fig. 5)

Maxilla with six functional (12 total) on right and seven (14 total) on left teeth. All the teeth subequal, lacking a distinct diastema. Pterygoid with total of 6–7 teeth. Palatine with 13–14 functional (24–25 total) teeth that gradually decrease in size posteriorly. Mandibles with 21 and 23 (more than 50 total) functional dentary teeth of left and right, respectively.

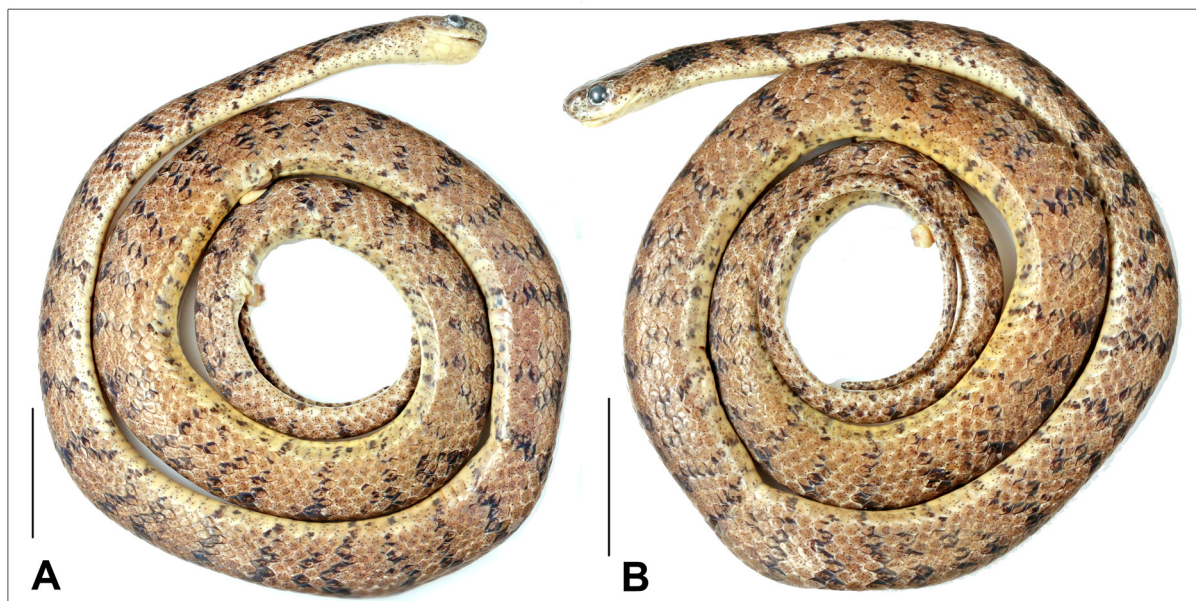


Fig. 2. *Pareas kaduri* sp. nov. Holotype, ♂ (BNHS 3574). A–B. Lateral views. Scale bars = 25 mm.

Variation shown by paratypes and referred specimens

The paratypes match the holotype in all respect except for the details noted herein: dorsal scales of female paratype BNHS 3575 are smooth, lacking keels, likely a character that is sexually dimorphic, in addition to fewer subcaudal scales. The color of individuals varies greatly in being light brown to dark blackish brown to reddish orange. Other differing characters are listed in Table 1.

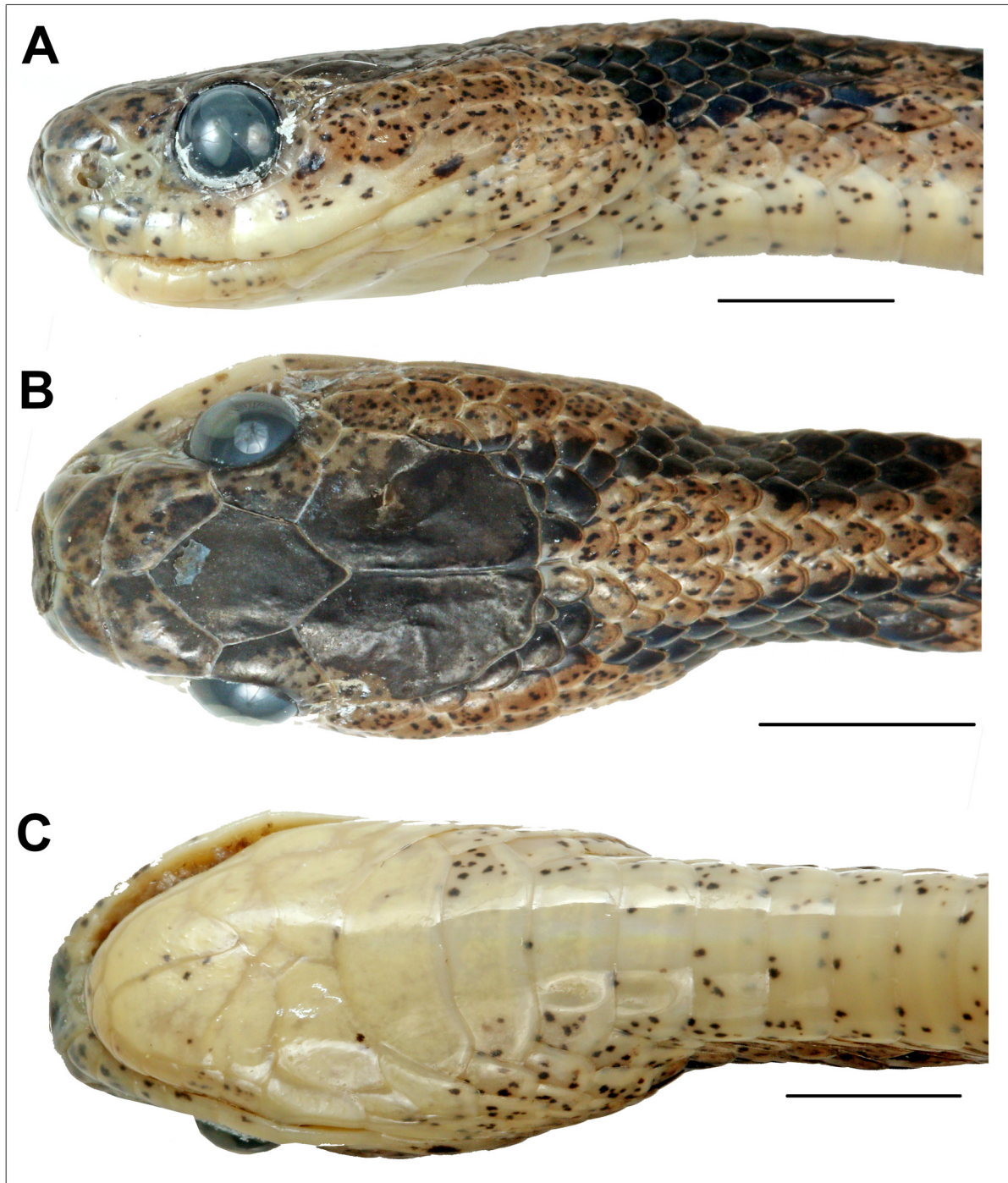


Fig. 3. *Pareas kaduri* sp. nov. Holotype, ♂ (BNHS 3574). View of head. A. Left lateral view. B. Dorsal view. C. Ventral view. Scale bars = 5 mm.

Table 1. Morphometric and meristic data for the type series of *Pareas kaduri* sp. nov.

	BNHS 3574	BNHS 3575	NCBS BH655	NCBS BH656	Range	Mean
Sex	♂	♀	♂	♂	–	–
TL	694	597	571	668	571–694	632.5
SVL	550	484	455	545	455–550	508.5
TaL	144	113	116	123	113–144	124
TaL/SVL	0.262	0.233	0.255	0.226	0.226–0.262	0.244
TaL/TL	0.207	0.189	0.203	0.184	0.184–0.207	0.196
HL	12	14.6	10.4	13.6	10.4–14.6	12.8125
CL	17.2	18.8	14.3	16.9	14.3–18.8	16.7
HW	8.8	6.8	7.1	7.9	7.1–8.8	7.3625
ED	3.5	3.6	2.7	3.2	2.7–3.6	3.25
EI	1.8	1.8	1.5	1.8	1.5–1.8	1.70625
ES	3.8	4.3	3.7	3.8	3.7–4.3	3.925
EN	2.5	2.3	2.3	2.7	2.3–2.7	2.4375
NW	4.6	5.8	3.5	4.3	3.5–5.8	4.5375
Ventrals	160	171	182	183	160–183	174
Subcaudals	70	52	70	65	52–70	64
DSR	15:15:15	15:15:15	15:15:15	15:15:15	–	–

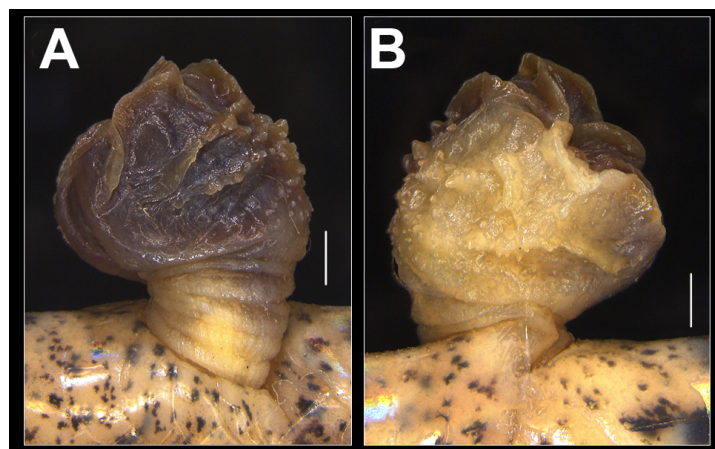


Fig. 4. *Pareas kaduri* sp. nov. Paratype, ♂ (NCBS BH655). A–B. Hemipenis, lateral view. Scale bars = 1 mm.

Genetic divergence

Interspecific divergence observed is 12–24% for *cyt b* and intraspecific genetic divergence is 1%. (Appendix 2).

Natural history

The type specimens were captured on low bushes along roads on the outskirts of Kamlang Wildlife Sanctuary at night. All the specimens were observed actively foraging after dusk. The habitat at the type locality is contiguous with the adjoining Namdapha Tiger Reserve and Mehao Wildlife Sanctuary, which lie in the Mishmi Hill range. Mishmi Hills lie between the Himalayas and the Indo-Burma biodiversity hotspot. The adjoining areas of Myanmar also share similar biotope and it is likely that the new species will be distributed in Myanmar in addition to India. The species was found in sympatry with *Pareas monticola*, *Boiga siamensis* Nutaphand, 1971, *Bungarus niger* Wall, 1908, *Ahetulla* sp. and *Trimeresurus popeiorum* Smith, 1937. The new species is common throughout the sampled area ranging from an elevation of 300 m to 1200 m, whereas *P. monticola* appears to be rare and only a single specimen was found at lower elevation (< 300 m).

Distribution

Currently, the new species is known only from the type locality, a tropical wet evergreen forest.

Discussion

The phylogenetic relationships recovered in the present work based on 1117 bp of mitochondrial cytochrome b gene (Fig. 6) are congruent with those of other studies (You *et al.* 2015; Zaher *et al.* 2019; Vogel *et al.* 2020; Wang *et al.* 2020), in which the new species, *P. kaduri* sp. nov., is sister to the clade containing *P. hamptoni*, *P. formosensis* and *P. mengziensis* with high support (ML bootstrap 89, BI posterior probability 0.99). The new species differs from *P. hamptoni* and *P. mengziensis* in exhibiting an uncorrected pairwise sequence divergence of 12% (Appendix 2). From other congeners,

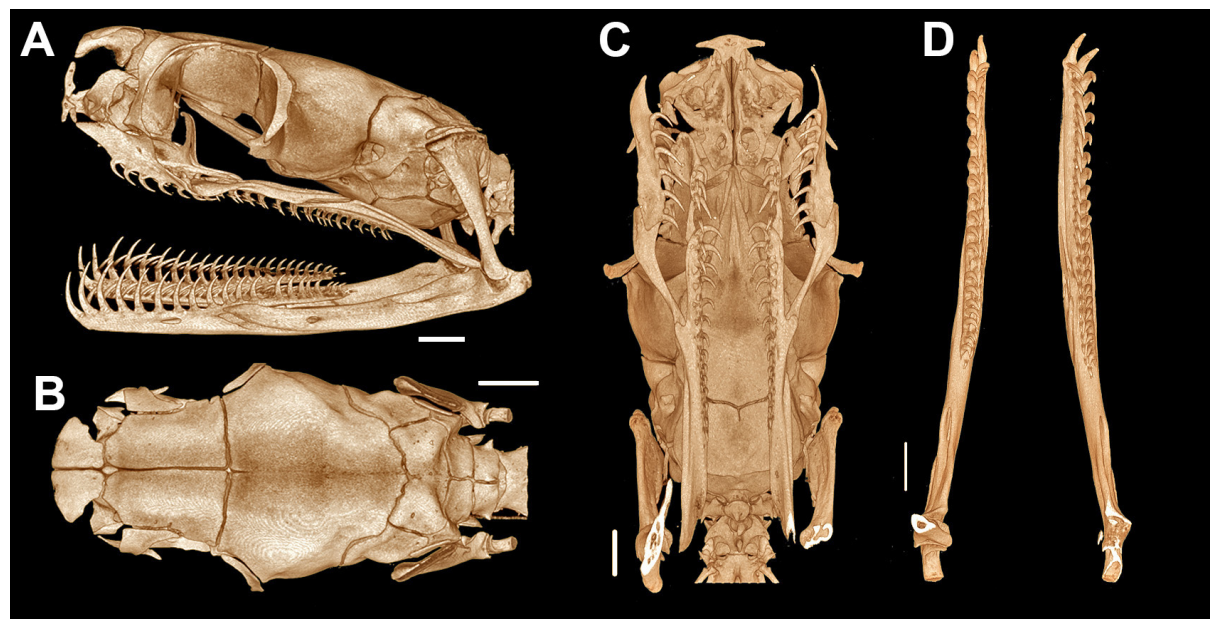


Fig. 5. *Pareas kaduri* sp. nov. Holotype, ♂ (BNHS 3574). Micro-CT scans of the head. **A.** Left lateral view. **B.** Dorsal view. **C.** Ventral view, without mandibles. **D.** Dorsal view of mandibles. Scale bars = 1 mm.

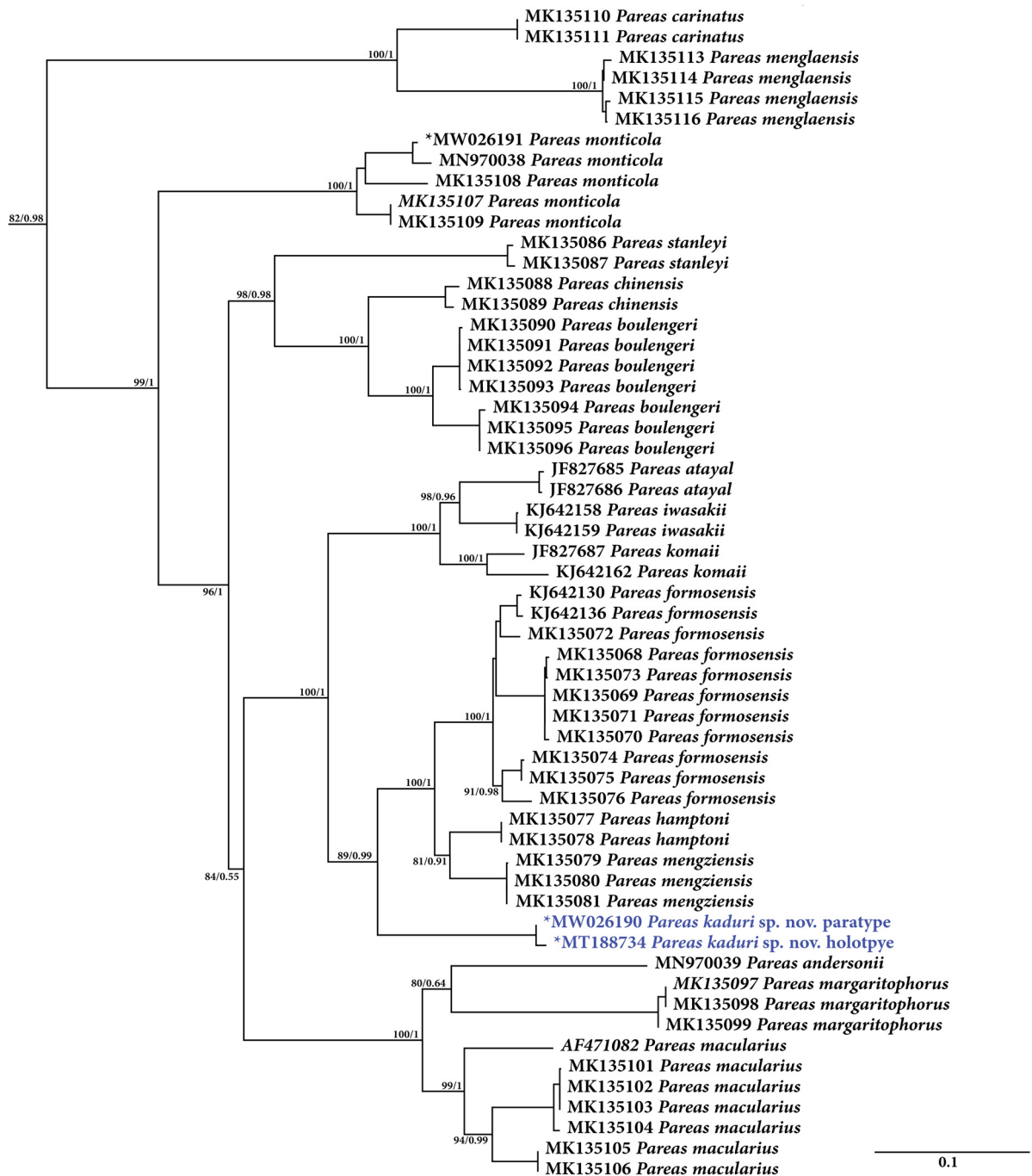


Fig. 6. ML phylogeny of *Pareas* based on partial sequences of the mitochondrial *cyt b* gene generated through 1000 non-parametric bootstrap pseudoreplicates under the GTR + G model of sequence evolution. Numbers at nodes represent ML bootstrap support and BI posterior probability. For a complete tree see Appendix III.

the new species shows an un-corrected p-distance of 13–24% (Appendix 2). The molecular phylogeny based on 16S rRNA recovered similar relationships (Appendix 4). The genetic data hint at the presence of undocumented diversity within *Pareas*, especially in the broadly distributed species of the genus (see Vogel *et al.* 2020). Further work on the widespread members of *Pareas* must be undertaken to ascertain the taxonomic status of genetically distinct lineages. Discovery of the new species of *Pareas* of the *P. hamptoni* clade is the first record of a member of this clade in India and the basal relationship of the species in it hints at a Himalayan origin of the clade. Our work brings the total number of species recognized within the genus *Pareas* to 20.

The discovery of yet another snake species from the same expedition to Arunachal Pradesh, after *Trachischium apteii* Bhosale, Gowande & Mirza, 2019 (Bhosale *et al.* 2019) and *Trimeresurus salazar* Mirza, Bhosale, Phansalkar, Sawant, Gowande & Patel, 2020 (Mirza *et al.* 2020), is not surprising as this region has received less attention in terms of documentation of diversity of reptiles. These discoveries advocate the need for extensive exploration across northeast India as a whole, to document the diversity of reptiles and perhaps other poorly studied taxa. Large expanses of forested habitats outside protected areas are under severe anthropogenic pressure and efforts must be made to safeguard these habitats especially in Arunachal Pradesh.

Acknowledgments

We thank the Forest Department of Arunachal Pradesh for issuing the necessary permits (Permit nos. CWL/Gen/173/2018-19/Pt.V11/2434-43 to ZM and CWL/Gen/173/2018-19/Pt.V11/2421-33 to GG) to conduct surveys across the state. Singinawa Conservation Foundation supported ZAM and Shripad Halbe (Brihad Bharatiya Samaj) supported HB and his team. We also thank Deepak Apte and Rahul Khot (BNHS) for his constant support. GG was supported by the Rufford Small Grants for Nature Conservation, for research on Indian agamids. GG is indebted to the Principal, Abasaheb Garware College, to the HoD, Annasaheb Kulkarni Department of Biodiversity, Abasaheb Garware College, and to the Principal, Fergusson College, and to the HoD, Biotechnology, Fergusson College and his advisor Dhanashree Paranjpe, for their constant support and encouragement. ZM thanks K. VijayRaghavan for guidance and all lab mates for their support. ZM wishes to acknowledge Kaushik Deuti (ZSI, Kolkata), Patrick Campbell (NHMUK, London), Nicholas Vidal (MNHN, Paris) for access to specimens and logistical support. Visit to museums would not have been possible without the help of the Infosys Travel Grant. Special thanks to an anonymous reviewer and Nikolay A. Poyarkov for their comments from which the manuscript greatly benefitted.

Authors' contributions

ZAM, HP, HB and GG designed the study; HB, PP, MS, GG and ZAM conducted fieldwork; ZAM and GG performed molecular analysis; ZAM, HP and GG wrote the paper. All authors read and approved the final manuscript.

Disclosure statement

No conflict of interest exists.

Funding

The work was supported by Singinawa Conservation Foundation, Shripad Halbe (Brihad Bharatiya Samaj) and The Rufford Foundation.

References

Anonymous 2015. The Deep Scaly Project, 2015, "*Pareas hamptoni*", Digital Morpholog. Available from http://digimorph.org/specimens/Pareas_hamptoni/ [accessed 26 Nov. 2019].

- Bhosale H.S., Gowande G. & Mirza Z.A. 2019. New species of fossorial natricid snakes of the genus *Trachischium* Günther, 1858 (Serpentes: Natricidae) from the Himalayas of northeast India. *Comptes Rendus Biologies* 342: 323–329. <https://doi.org/10.1016/j.crvi.2019.10.003>
- Deepak V., Ruane S. & Gower D.J. 2018. A new subfamily of fossorial colubroid snakes from the Western Ghats of peninsular India. *Journal of Natural History* 52: 2919–2934. <https://doi.org/10.1080/00222933.2018.1557756>
- Dowling H. 1951. A proposed standard system of counting ventrals in snakes. *British Journal of Herpetology* 11: 97–99.
- Heatwole H. 2009. *Biology of the Reptilia. Volume 20, Morphology H, The Skull of Lepidosauria*. Carl Gans, Abbot S. Gaunt, and Kraig Adler, editors. *Integrative and Comparative Biology* 49: 610–611. <https://doi.org/10.1093/icb/icp063>
- Hoso M., Asami T. & Hori M. 2007. Right-handed snakes: convergent evolution of asymmetry for functional specialization. *Biology Letters* 3: 169–172. <https://doi.org/10.1098/rsbl.2006.0600>
- Kumar S., Stecher G., Li M., Knyaz C. & Tamura K. 2018. MEGA X: Molecular Evolutionary Genetics Analysis across computing platforms. *Molecular Biology and Evolution* 35: 1547–1549. <https://doi.org/10.1093/molbev/msy096>
- Lalbiakzuala & Lalremsanga H.T. 2019. *Pareas margaritophorus*, a new country report for India. *Herpetological Review* 50: 332.
- Lanfear R., Calcott B., Ho S. & Guindon S. 2012. PartitionFinder: combined selection of partitioning schemes and substitution models for phylogenetic analyses. *Molecular Biology and Evolution* 29: 1695–1701. <https://doi.org/10.1093/molbev/mss020>
- Leary S., Underwood W., Anthony R. & Cartner S. 2013. *AVMA Guidelines for the Euthanasia of Animals: 2013 edition*. American Veterinary Medical Association, Schaumburg, IL, USA.
- Mirza Z.A. & Patel H. 2018. Back from the dead! Resurrection and revalidation of the Indian endemic snake genus *Wallophis* Werner, 1929 (Squamata: Colubridae) insights from molecular data. *Mitochondrial DNA Part A: DNA Mapping, Sequencing, and Analysis* 29: 331–334. <https://doi.org/10.1080/24701394.2016.1278536>
- Mirza Z.A., Vyas R., Patel H., Maheta J. & Sanap R.V. 2016. A new Miocene-divergent lineage of Old World racer snake from India. *PloS ONE* 11 (3): e0148380. <https://doi.org/10.1371/journal.pone.0148380>
- Mirza Z.A., Bhosale H.S., Phansalkar P.U., Sawant M., Gowande G.G. & Patel H. 2020. A new species of green pit vipers of the genus *Trimeresurus* Lacépède, 1804 (Reptilia: Serpentes: Viperidae) from western Arunachal Pradesh, India. *Zoosystematics and Evolution* 96: 123–138. <https://doi.org/10.3897/zse.96.48431>
- Pyron R.A., Kandambi H.K.D., Hendry C.R., Pushpamal V., Burbrink F.T. & Somaweera R. 2013. Genus-level phylogeny of snakes reveals the origins of species richness in Sri Lanka. *Molecular Phylogenetics and Evolution* 66: 969–978. <https://doi.org/10.1016/j.ympev.2012.12.004>
- Ronquist F. & Huelsenbeck J. 2003. MrBayes 3: Bayesian phylogenetic inference under mixed models. *Bioinformatics* 19: 1572–1574. <https://doi.org/10.1093/bioinformatics/btg180>
- Thompson J.D., Gibson T.J. & Higgins D.G. 2002. Multiple sequence alignment using ClustalW and ClustalX. *Current Protocols in Bioinformatics* 0: 2.3.1–2.3.22. <https://doi.org/10.1002/0471250953.bi0203s00>

- Trifinopoulos J., Nguyen L., von Haeseler A. & Minh B.Q. 2016. W-IQ-TREE: a fast online phylogenetic tool for maximum likelihood analysis. *Nucleic Acids Research* 44: W232–W235. <https://doi.org/10.1093/nar/gkw256>
- Vitt L.J. & Caldwell J.P. 2014. Chapter 2 - Anatomy of Amphibians and Reptiles. *In*: Vitt L.J. & Caldwell J.P. (eds) *Herpetology: An Introductory Biology of Amphibians and Reptiles*: 35–82. Academic Press, San Diego. <https://doi.org/10.1016/B978-0-12-386919-7.00002-2>
- Vogel G. 2015. A new montane species of the genus *Pareas* Wagler, 1830 (Squamata: Pareasidae) from Northern Myanmar. *TAPROBANICA: The Journal of Asian Biodiversity* 7: 1–7. <https://doi.org/10.4038/tapro.v7i1.7501>
- Vogel G., Nguyen T. van, Lalremsanga H.T., Biakzuala L., Hrima V. & Poyarkov N.A. 2020. Taxonomic reassessment of the *Pareas margaritiferus-macularius* species complex (Squamata, Pareasidae). *Vertebrate Zoology* 70: 547–569. <https://doi.org/10.26049/VZ70-4-2020-02>
- Wallach V., Williams K.L. & Boundy J. 2014. *Snakes of the World: A Catalogue of Living and Extinct Species*. Taylor & Francis Group, London. <https://doi.org/10.1201/b16901>
- Wang P., Che J., Liu Q., Li K., Jin J.Q., Jiang K., Shi L. & Guo P. 2020. A revised taxonomy of Asian snail-eating snakes *Pareas* (Squamata, Pareasidae): evidence from morphological comparison and molecular phylogeny. *ZooKeys* 939: 45–64. <https://doi.org/10.3897/zookeys.939.49309>
- Whitaker R. & Captain A. 2004. *Snakes of India. The Field Guide*. Draco Books, Chennai.
- You C.W., Poyarkov N.A. & Lin S.M. 2015. Diversity of the snail-eating snakes *Pareas* (Serpentes, Pareasidae) from Taiwan. *Zoologica Scripta* 44: 349–361. <https://doi.org/10.1111/zsc.12111>
- Zaher H., Murphy R.W., Arredondo J.C., Graboski R., Machado-Filho P.R., Mahlow K., Montingelli G.G., Quadros A.B., Orlov N.L., Wilkinson M., Zhang Y.P. & Grazziotin F.G. 2019. Large-scale molecular phylogeny, morphology, divergence-time estimation, and the fossil record of advanced caenophidian snakes (Squamata: Serpentes). *PLoS ONE* 14 (5): e0216148. <https://doi.org/10.1371/journal.pone.0216148>

Manuscript received: 5 July 2020

Manuscript accepted: 25 October 2020

Published on: 17 December 2020

Topic editor: Rudy Jocqué

Desk editor: Pepe Fernández

Printed versions of all papers are also deposited in the libraries of the institutes that are members of the *EJT* consortium: Muséum national d'histoire naturelle, Paris, France; Meise Botanic Garden, Belgium; Royal Museum for Central Africa, Tervuren, Belgium; Royal Belgian Institute of Natural Sciences, Brussels, Belgium; Natural History Museum of Denmark, Copenhagen, Denmark; Naturalis Biodiversity Center, Leiden, the Netherlands; Museo Nacional de Ciencias Naturales-CSIC, Madrid, Spain; Real Jardín Botánico de Madrid CSIC, Spain; Zoological Research Museum Alexander Koenig, Bonn, Germany; National Museum, Prague, Czech Republic.

Appendix 1 (continued on next page). Details of species and accession numbers used in the present work based on Wang *et al.* (2020).

Taxon	Voucher number	Locality	GenBank accession number
<i>Pareas formosensis</i>	YBU 12015	Hainan, China	MK135068
<i>P. formosensis</i>	GP 2164	Hainan, China	MK135069
<i>P. formosensis</i>	GP 2165	Hainan, China	MK135070
<i>P. formosensis</i>	YBU 12032	Hainan, China	MK135071
<i>P. formosensis</i>	GP 4581	Jingning, Zhejiang, China	MK135072
<i>P. formosensis</i>	YBU 17029	Hainan, China	MK135073
<i>P. formosensis</i>	YBU 12090	Leishan, Guizhou, China	MK135074
<i>P. formosensis</i>	YBU 12115	Rongjiang, Guizhou, China	MK135075
<i>P. formosensis</i>	YBU 14508	Guangxi, China	MK135076
<i>P. formosensis</i>	GP 3696	Yanshan, Jiangxi, China	HM46857
<i>P. formosensis</i>	GP 3808	Yanshan, Jiangxi, China	HM46858
<i>P. formosensis</i>	YBU 14573	Yanshan, Jiangxi, China	HM46859
<i>P. formosensis</i>	NMNS 05632	N. Cross-Is. Highway, Taiwan, China	KJ642130
<i>P. formosensis</i>	NMNS 05637	Xitou, Nantou, Taiwan, China	KJ642136
<i>P. hamptoni</i>	YPX 18219	Myanmar	MK135077
<i>P. hamptoni</i>	YPX 18604	Myanmar	MK135078
<i>P. mengziensis</i>	GP 1294	Mengzi, Yunnan, China	MK135079
<i>P. mengziensis</i>	YBU 14251	Mengzi, Yunnan, China	MK135080
<i>P. mengziensis</i>	YBU 14252	Mengzi, Yunnan, China	MK135081
<i>P. mengziensis</i>	YBU 14253	Mengzi, Yunnan, China	MK135082
<i>P. mengziensis</i>	YBU 14288	Mengzi, Yunnan, China	MK135083
<i>P. mengziensis</i>	YBU 15100	Kaiyuan, Yunnan, China	MK135084
<i>P. mengziensis</i>	YBU 15114	Kaiyuan, Yunnan, China	MK135085
<i>P. stanleyi</i>	GP 229	Guangxi, China	MK135086
<i>P. stanleyi</i>	YBU 12094	Leishan, Guizhou, China	MK135087
<i>P. chinensis</i>	GP 2196	Junlian, Sichuan, China	MK135088
<i>P. chinensis</i>	GP 2383	Hongya, Sichuan, China	MK135089
<i>P. boulengeri</i>	GP 2923	Jiangkou, Guizhou, China	MK135090
<i>P. boulengeri</i>	GP 207	Anxian, Sichuan, China	MK135091
<i>P. boulengeri</i>	YBU 13323A	Wufeng, Hubei, China	MK135092
<i>P. boulengeri</i>	GP 4716	Yidu, Hubei, China	MK135093
<i>P. boulengeri</i>	GP 3428	Yixian, Anhui, China	MK135094
<i>P. boulengeri</i>	YBU 17155	Chunan, Zhejiang, China	MK135095
<i>P. boulengeri</i>	YBU 17245	Chunan, Zhejiang, China	MK135096
<i>P. margaritophorus</i>	YBU 16061	Cangwu, Guangxi, China	MK135097
<i>P. margaritophorus</i>	YBU 17164	Cangwu, Guangxi, China	MK135098
<i>P. margaritophorus</i>	GP 4437	Cangwu, Guangxi, China	MK135099
<i>P. margaritophorus</i>	YBU 16095	Cangwu, Guangxi, China	MK135100
<i>P. macularius</i>	GP815	Hainan, China	MK135101

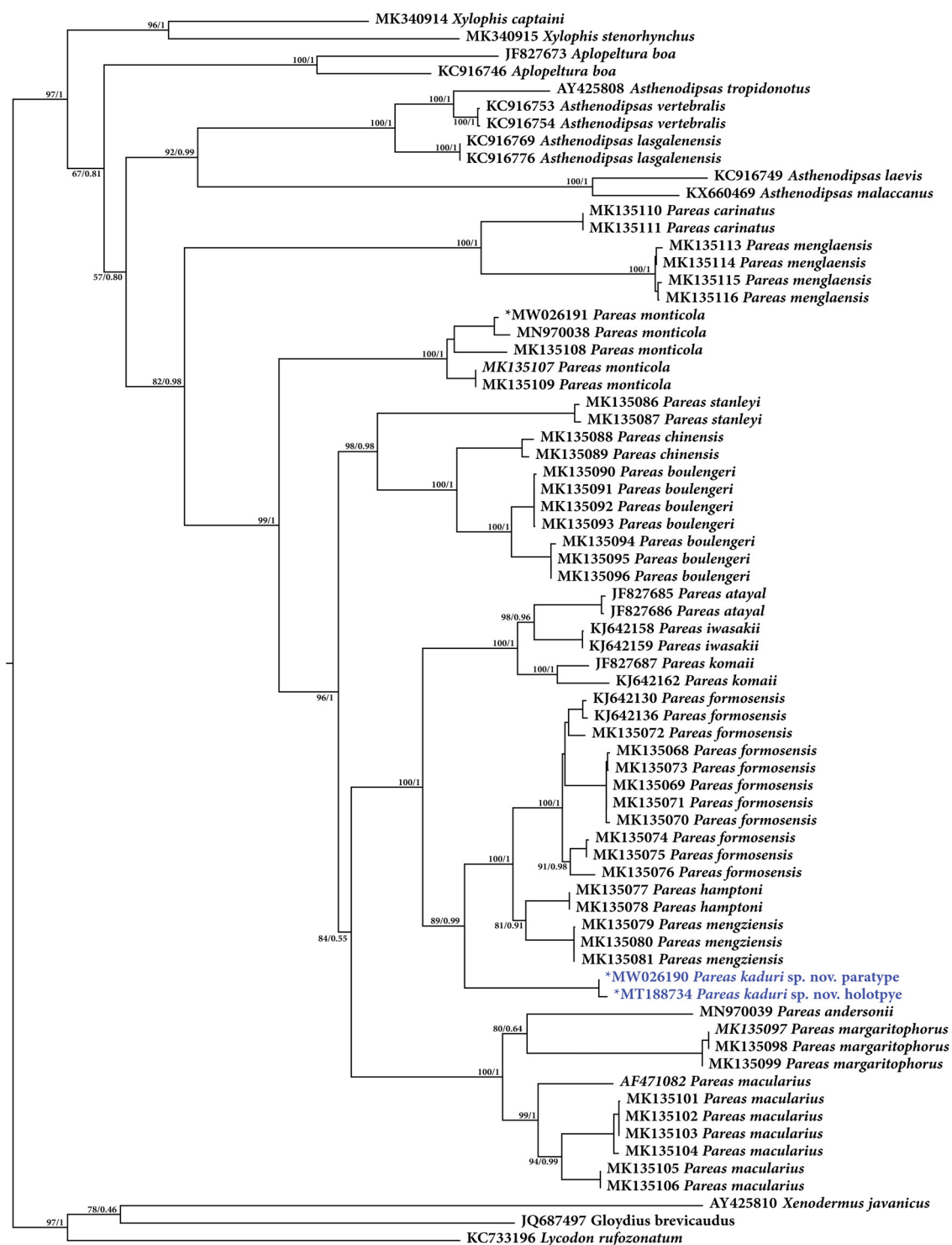
Appendix 1 (continued).

Taxon	Voucher number	Locality	GenBank accession number
<i>P. macularius</i>	GP 2110	Hainan, China	MK135102
<i>P. macularius</i>	YBU 12016	Hainan, China	MK135103
<i>P. macularius</i>	YBU 17030	Hainan, China	MK135104
<i>P. macularius</i>	YBU 17078	Jingdong, Yunnan, China	MK135105
<i>P. macularius</i>	YBU 17062	Jingdong, Yunnan, China	MK135106
<i>P. monticola</i>	GP 2027	Motuo, Xizang, China	MK135107
<i>P. monticola</i>	KIZ 047036	Pingbian, Yunnan, China	MK135108
<i>P. monticola</i>	KIZ 014167	Motuo, Xizang, China	MK135109
<i>P. carinatus</i>	GP 1079	Malaysia	MK135110
<i>P. carinatus</i>	KIZ 011972	Malaysia	MK135111
<i>P. carinatus</i>	KIZ 011970	Malaysia	MK135112
<i>P. menglaensis</i>	GP 1292	Mengla, Yunnan, China	MK135113
<i>P. menglaensis</i>	YBU 14124	Mengla, Yunnan, China	MK135114
<i>P. menglaensis</i>	YBU 14141	Mengla, Yunnan, China	MK135115
<i>P. menglaensis</i>	YBU 14142	Mengla, Yunnan, China	MK135116
<i>P. atayal</i> 1	HC 000618	N. Cross-Is. Highway, Taiwan, China	JF827685
<i>P. atayal</i> 2	HC 000628	N. Cross-Is. Highway, Taiwan, China	JF827686
<i>P. komaii</i> 1	HC 000669	Lijia, Taidong, Taiwan, China	JF827687
<i>P. komaii</i> 2	NMNS 05598	Daxueshan, Taichung, Taiwan, China	KJ642162
<i>P. iwesakii</i> 1	I03-ISG1	Ishigaki Is., S. Ryukyu, Japan	KJ642158
<i>P. iwesakii</i> 2	I04-ISG2	Ishigaki Is., S. Ryukyu, Japan	KJ642159
<i>P. macularius</i>	CAS 206620	Bago Division, Myanmar	AF471082
<i>Aplopeltura boa</i> 1	KIZ 011963	Malaysia	JF827673
<i>A. boa</i> 2	LSUHC 7248	Malaysia	KC916746
<i>Asthenodipsas laevis</i>	LSUHC 10346	Peninsular Malaysia	KC916749
<i>A. malaccanus</i>	FMNH 273617	–	KX660469
<i>A. vertebralis</i> 1	LSUHC 9138	Peninsular Malaysia	KC916754
<i>A. vertebralis</i> 2	LSUHC 9873	Peninsular Malaysia	KC916753
<i>A. lasgalenensis</i> 1	10668	Peninsular Malaysia	KC916776
<i>A. lasgalenensis</i> 2	7228	Peninsular Malaysia	KC916769
<i>A. tropidonotus</i>		Sumatra, Indonesia	AY425808
<i>X. stenorhynchus</i>	CAS 17199	India	MK340915
<i>X. captaini</i>	BNHS 3376	Kottayam, Kerala, India	MK340914
<i>Lycodon rufozonatum</i>	GP 625	Dandong, Liaoning, China	KC733196
<i>Gloydium brevicaudus</i>	GP1099	Dalian, Liaoning, China	JQ687497
<i>Xenodermus javanicus</i>	FMNH 230073	Malaysia	AY425810

Appendix 2. Un-corrected pairwise divergence (p-distance) for *Pareas* spp. based on mitochondrial *cyt b* gene.

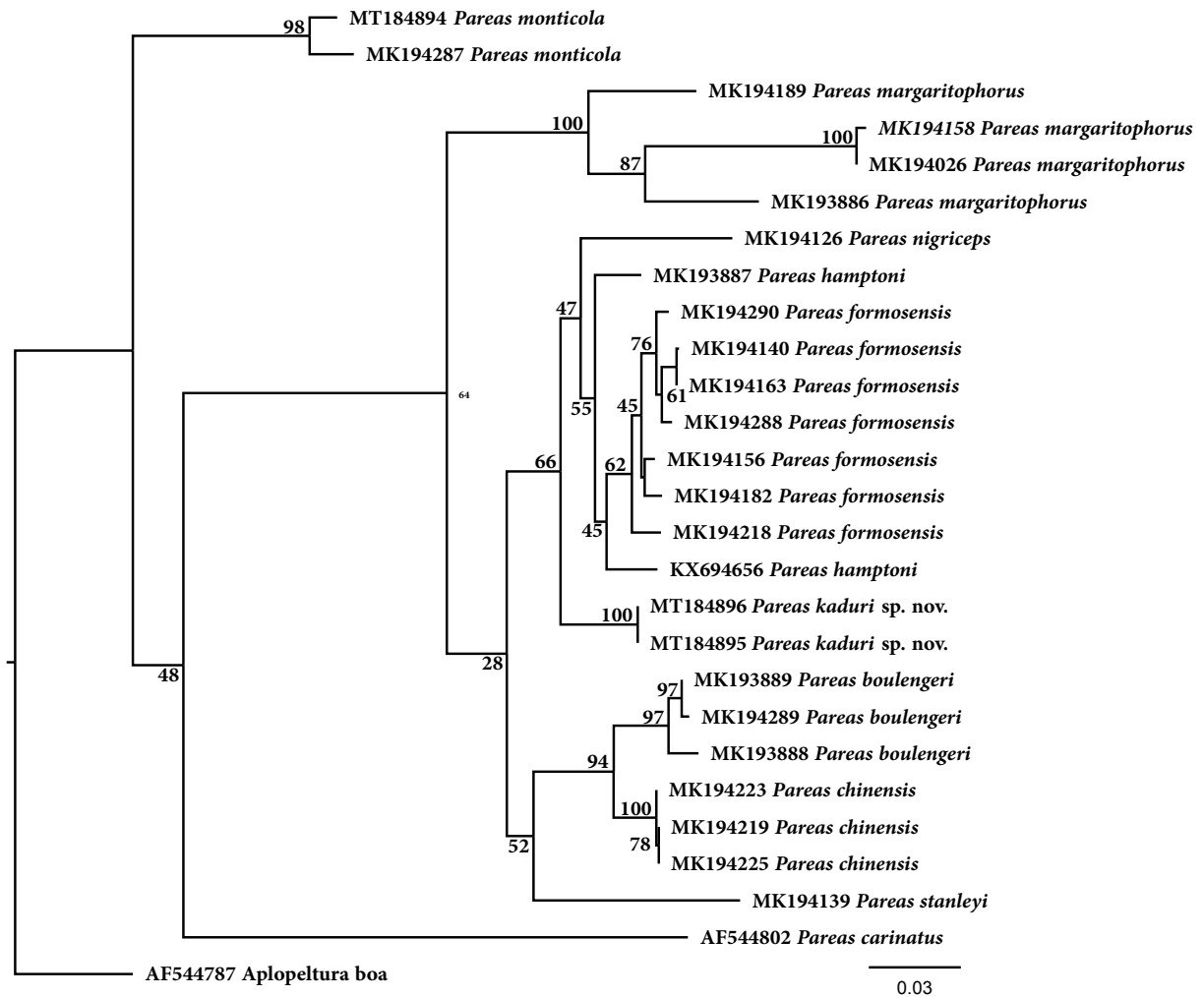
1	MF178724	<i>Pareas kaduif</i> sp. nov.	0.19	0.00
2	ZM1917	<i>Pareas kaduif</i> sp. nov.	0.18	0.09
3	MK135115	<i>Pareas mengalensis</i>	0.17	0.18
4	MK135114	<i>Pareas mengalensis</i>	0.17	0.18
5	MK135112	<i>Pareas carnatus</i>	0.17	0.18
6	MK135110	<i>Pareas carnatus</i>	0.17	0.18
7	MK135109	<i>Pareas monticola</i>	0.17	0.18
8	MK135108	<i>Pareas monticola</i>	0.17	0.18
9	MK135107	<i>Pareas mangarophorus</i>	0.17	0.18
10	MK135106	<i>Pareas mangarophorus</i>	0.17	0.18
11	MK135105	<i>Pareas mangarophorus</i>	0.17	0.18
12	MK135104	<i>Pareas mangarophorus</i>	0.17	0.18
13	MK135103	<i>Pareas mangarophorus</i>	0.17	0.18
14	MK135102	<i>Pareas mangarophorus</i>	0.17	0.18
15	MK135101	<i>Pareas mangarophorus</i>	0.17	0.18
16	MK135098	<i>Pareas mangarophorus</i>	0.17	0.18
17	MK135097	<i>Pareas boulangeri</i>	0.17	0.18
18	MK135096	<i>Pareas boulangeri</i>	0.17	0.18
19	MK135095	<i>Pareas boulangeri</i>	0.17	0.18
20	MK135094	<i>Pareas boulangeri</i>	0.17	0.18
21	MK135093	<i>Pareas boulangeri</i>	0.17	0.18
22	MK135092	<i>Pareas boulangeri</i>	0.17	0.18
23	MK135091	<i>Pareas boulangeri</i>	0.17	0.18
24	MK135089	<i>Pareas chrenensis</i>	0.17	0.18
25	MK135088	<i>Pareas chrenensis</i>	0.17	0.18
26	MK135087	<i>Pareas stahleyi</i>	0.17	0.18
27	MK135086	<i>Pareas stahleyi</i>	0.17	0.18
28	MK135085	<i>Pareas hamptoni</i>	0.17	0.18
29	MK135084	<i>Pareas hamptoni</i>	0.17	0.18
30	MK135083	<i>Pareas hamptoni</i>	0.17	0.18
31	MK135082	<i>Pareas hamptoni</i>	0.17	0.18
32	MK135081	<i>Pareas hamptoni</i>	0.17	0.18
33	MK135080	<i>Pareas mengalensis</i>	0.17	0.18
34	MK135079	<i>Pareas mengalensis</i>	0.17	0.18
35	MK135078	<i>Pareas hamptoni</i>	0.17	0.18
36	MK135077	<i>Pareas cf. tonkensis</i>	0.17	0.18
37	MK135076	<i>Pareas cf. tonkensis</i>	0.17	0.18
38	MK135075	<i>Pareas cf. tonkensis</i>	0.17	0.18
39	MK135074	<i>Pareas cf. tonkensis</i>	0.17	0.18
40	MK135073	<i>Pareas tonkensis</i>	0.17	0.18
41	MK135072	<i>Pareas tonkensis</i>	0.17	0.18
42	MK135071	<i>Pareas tonkensis</i>	0.17	0.18
43	MK135070	<i>Pareas tonkensis</i>	0.17	0.18
44	MK135069	<i>Pareas tonkensis</i>	0.17	0.18
45	MK135068	<i>Pareas tonkensis</i>	0.17	0.18
46	KJ62162	<i>Pareas kornali</i>	0.17	0.18
47	KJ62159	<i>Pareas waskeli</i>	0.17	0.18
48	KJ62158	<i>Pareas waskeli</i>	0.17	0.18
49	KJ62136	<i>Pareas hamptoni</i>	0.17	0.18
50	KJ62130	<i>Pareas hamptoni</i>	0.17	0.18
51	MN77039	<i>Pareas monticola</i>	0.17	0.18
52	ZM131	<i>Pareas tonkensis</i>	0.17	0.18
53	AV42506	<i>Pareas tonkensis</i>	0.17	0.18
54	JF82767	<i>Pareas kornali</i>	0.17	0.18
55	JF82766	<i>Pareas stahleyi</i>	0.17	0.18
56	JF82765	<i>Pareas stahleyi</i>	0.17	0.18
57	AF471082	<i>Pareas maculatus</i>	0.19	0.10
58	MK135065	<i>Pareas maculatus</i>	0.19	0.10
59	MK135064	<i>Pareas maculatus</i>	0.19	0.10
60	MK135063	<i>Pareas maculatus</i>	0.19	0.10
61	MK135062	<i>Pareas maculatus</i>	0.19	0.10
62	MK135061	<i>Pareas maculatus</i>	0.19	0.10
63	MK135060	<i>Pareas maculatus</i>	0.19	0.10
64	MK135059	<i>Pareas maculatus</i>	0.19	0.10
65	MK135058	<i>Pareas maculatus</i>	0.19	0.10
66	MK135057	<i>Pareas maculatus</i>	0.19	0.10
67	MK135056	<i>Pareas maculatus</i>	0.19	0.10
68	MK135055	<i>Pareas maculatus</i>	0.19	0.10
69	MK135054	<i>Pareas maculatus</i>	0.19	0.10
70	MK135053	<i>Pareas maculatus</i>	0.19	0.10
71	MK135052	<i>Pareas maculatus</i>	0.19	0.10
72	MK135051	<i>Pareas maculatus</i>	0.19	0.10
73	MK135050	<i>Pareas maculatus</i>	0.19	0.10
74	MK135049	<i>Pareas maculatus</i>	0.19	0.10
75	MK135048	<i>Pareas maculatus</i>	0.19	0.10
76	MK135047	<i>Pareas maculatus</i>	0.19	0.10
77	MK135046	<i>Pareas maculatus</i>	0.19	0.10
78	MK135045	<i>Pareas maculatus</i>	0.19	0.10
79	MK135044	<i>Pareas maculatus</i>	0.19	0.10
80	MK135043	<i>Pareas maculatus</i>	0.19	0.10
81	MK135042	<i>Pareas maculatus</i>	0.19	0.10
82	MK135041	<i>Pareas maculatus</i>	0.19	0.10
83	MK135040	<i>Pareas maculatus</i>	0.19	0.10
84	MK135039	<i>Pareas maculatus</i>	0.19	0.10
85	MK135038	<i>Pareas maculatus</i>	0.19	0.10
86	MK135037	<i>Pareas maculatus</i>	0.19	0.10
87	MK135036	<i>Pareas maculatus</i>	0.19	0.10
88	MK135035	<i>Pareas maculatus</i>	0.19	0.10
89	MK135034	<i>Pareas maculatus</i>	0.19	0.10
90	MK135033	<i>Pareas maculatus</i>	0.19	0.10
91	MK135032	<i>Pareas maculatus</i>	0.19	0.10
92	MK135031	<i>Pareas maculatus</i>	0.19	0.10
93	MK135030	<i>Pareas maculatus</i>	0.19	0.10
94	MK135029	<i>Pareas maculatus</i>	0.19	0.10
95	MK135028	<i>Pareas maculatus</i>	0.19	0.10
96	MK135027	<i>Pareas maculatus</i>	0.19	0.10
97	MK135026	<i>Pareas maculatus</i>	0.19	0.10
98	MK135025	<i>Pareas maculatus</i>	0.19	0.10
99	MK135024	<i>Pareas maculatus</i>	0.19	0.10
100	MK135023	<i>Pareas maculatus</i>	0.19	0.10
101	MK135022	<i>Pareas maculatus</i>	0.19	0.10
102	MK135021	<i>Pareas maculatus</i>	0.19	0.10
103	MK135020	<i>Pareas maculatus</i>	0.19	0.10
104	MK135019	<i>Pareas maculatus</i>	0.19	0.10
105	MK135018	<i>Pareas maculatus</i>	0.19	0.10
106	MK135017	<i>Pareas maculatus</i>	0.19	0.10
107	MK135016	<i>Pareas maculatus</i>	0.19	0.10
108	MK135015	<i>Pareas maculatus</i>	0.19	0.10
109	MK135014	<i>Pareas maculatus</i>	0.19	0.10
110	MK135013	<i>Pareas maculatus</i>	0.19	0.10
111	MK135012	<i>Pareas maculatus</i>	0.19	0.10
112	MK135011	<i>Pareas maculatus</i>	0.19	0.10
113	MK135010	<i>Pareas maculatus</i>	0.19	0.10
114	MK135009	<i>Pareas maculatus</i>	0.19	0.10
115	MK135008	<i>Pareas maculatus</i>	0.19	0.10
116	MK135007	<i>Pareas maculatus</i>	0.19	0.10
117	MK135006	<i>Pareas maculatus</i>	0.19	0.10
118	MK135005	<i>Pareas maculatus</i>	0.19	0.10
119	MK135004	<i>Pareas maculatus</i>	0.19	0.10
120	MK135003	<i>Pareas maculatus</i>	0.19	0.10
121	MK135002	<i>Pareas maculatus</i>	0.19	0.10
122	MK135001	<i>Pareas maculatus</i>	0.19	0.10
123	MK135000	<i>Pareas maculatus</i>	0.19	0.10
124	MK134999	<i>Pareas maculatus</i>	0.19	0.10
125	MK134998	<i>Pareas maculatus</i>	0.19	0.10
126	MK134997	<i>Pareas maculatus</i>	0.19	0.10
127	MK134996	<i>Pareas maculatus</i>	0.19	0.10
128	MK134995	<i>Pareas maculatus</i>	0.19	0.10
129	MK134994	<i>Pareas maculatus</i>	0.19	0.10
130	MK134993	<i>Pareas maculatus</i>	0.19	0.10
131	MK134992	<i>Pareas maculatus</i>	0.19	0.10
132	MK134991	<i>Pareas maculatus</i>	0.19	0.10
133	MK134990	<i>Pareas maculatus</i>	0.19	0.10
134	MK134989	<i>Pareas maculatus</i>	0.19	0.10
135	MK134988	<i>Pareas maculatus</i>	0.19	0.10
136	MK134987	<i>Pareas maculatus</i>	0.19	0.10
137	MK134986	<i>Pareas maculatus</i>	0.19	0.10
138	MK134985	<i>Pareas maculatus</i>	0.19	0.10
139	MK134984	<i>Pareas maculatus</i>	0.19	0.10
140	MK134983	<i>Pareas maculatus</i>	0.19	0.10
141	MK134982	<i>Pareas maculatus</i>	0.19	0.10
142	MK134981	<i>Pareas maculatus</i>	0.19	0.10
143	MK134980	<i>Pareas maculatus</i>	0.19	0.10
144	MK134979	<i>Pareas maculatus</i>	0.19	0.10
145	MK134978	<i>Pareas maculatus</i>	0.19	0.10
146	MK134977	<i>Pareas maculatus</i>	0.19	0.10
147	MK134976	<i>Pareas maculatus</i>	0.19	0.10
148	MK134975	<i>Pareas maculatus</i>	0.19	0.10
149	MK134974	<i>Pareas maculatus</i>	0.19	0.10
150	MK134973	<i>Pareas maculatus</i>	0.19	0.10
151	MK134972	<i>Pareas maculatus</i>	0.19	0.10
152	MK134971	<i>Pareas maculatus</i>	0.19	0.10
153	MK134970	<i>Pareas maculatus</i>	0.19	0.10
154	MK134969	<i>Pareas maculatus</i>	0.19	0.10
155	MK134968	<i>Pareas maculatus</i>	0.19	0.10
156	MK134967	<i>Pareas maculatus</i>	0.19	0.10
157	MK134966	<i>Pareas maculatus</i>	0.19	0.10
158	MK134965	<i>Pareas maculatus</i>	0.19	0.10
159	MK134964	<i>Pareas maculatus</i>	0.19	0.10
160	MK134963	<i>Pareas maculatus</i>	0.19	0.10
161	MK134962	<i>Pareas maculatus</i>	0.19	0.10
162	MK134961	<i>Pareas maculatus</i>	0.19	0.10
163	MK134960	<i>Pareas maculatus</i>	0.19	0.10
164	MK134959	<i>Pareas maculatus</i>	0.19	0.10
165	MK134958	<i>Pareas maculatus</i>	0.19	0.10
166	MK134957	<i>Pareas maculatus</i>	0.19	0.10
167	MK134956	<i>Pareas maculatus</i>	0.19	0.10
168	MK134955	<i>Pareas maculatus</i>	0.19	0.10
169	MK134954	<i>Pareas maculatus</i>	0.19	0.10
170	MK134953	<i>Pareas maculatus</i>	0.19	0.10
171	MK134952	<i>Pareas maculatus</i>	0.19	0.10
172	MK134951	<i>Pareas maculatus</i>	0.19	0.10
173	MK134950	<i>Pareas maculatus</i>	0.19	0.10
174	MK134949	<i>Pareas maculatus</i>	0.19	0.10
175	MK134948	<i>Pareas maculatus</i>	0.19	0.10
176	MK134947	<i>Pareas maculatus</i>	0.19	0.10
177	MK134946	<i>Pareas maculatus</i>	0.19	0.10
178	MK134945	<i>Pareas maculatus</i>	0.19	0.10
179	MK134944	<i>Pareas maculatus</i>	0.19	0.10
180	MK134943	<i>Pareas maculatus</i>	0.19	0.10
181	MK134942	<i>Pareas maculatus</i>	0.19	0.10
182	MK134941	<i>Pareas maculatus</i>	0.19	0.10
183	MK134940	<i>Pareas maculatus</i>	0.19	0.10
184	MK134939	<i>Pareas maculatus</i>	0.19	0.10
185	MK134938	<i>Pareas maculatus</i>	0.19	0.10
186	MK134937	<i>Pareas maculatus</i>	0.19	0.10
187	MK134936	<i>Pareas maculatus</i>	0.19	0.10
188	MK134935	<i>Pareas maculatus</i>	0.19	0.10
189	MK134934	<i>Pareas maculatus</i>	0.19	0.10
190	MK134933	<i>Pareas maculatus</i>	0.19	0.10
191	MK134932	<i>Pareas maculatus</i>	0.19	0.10
192	MK134931	<i>Pareas maculatus</i>	0.19	0.10
193	MK134930</			

Appendix 3. ML phylogeny of selected members of Pareinae Romer, 1956 based on partial sequences of mitochondrial *cyt b* gene generated through 1000 non-parametric bootstrap pseudoreplicates under the GTR + G model of sequence evolution. Numbers at nodes represent ML bootstrap support and BI posterior probability.



0.1

Appendix 4. ML phylogeny of selected members of Pareinae Romer, 1956 based on partial sequences of mitochondrial 16S rRNA gene generated through 1000 non-parametric bootstrap pseudoreplicates under the GTR + G model of sequence evolution. Numbers at nodes represent ML bootstrap support and BI posterior probability.



Appendix 5. Comparative material examined.

Pareas carinatus (Wagler, 1830) (= *Pareas berdmorei* Theobald, 1868)

MYANMAR • 2 specs, syntype; “Tenasserim” (in southern Myanmar); ZSI 8021, ZSI 8022.

Pareas hamptoni (Boulenger, 1905)

MYANMAR • 1 spec., Mogok, Upper Burma [= Myanmar]; NHMUK 1946.1.20.16 • 3 specs; Burma; NHMUK 1974.899, NHMUK 1974.231, NHMUK 1974.232.

CHINA • 1 spec.; Hainan; NHMUK 1937.2.1.18.

Pareas macularius Theobald, 1868

MYANMAR • 1 spec., syntype; “Tenasserim” [= Tanintharyi Div., S Myanmar]; NHMUK 1946.1.20.8.

Pareas monticola (Cantor, 1839)

INDIA • holotype; Asam, Naga Hills; NHMUK 1946.1.20.5 • 2 ♂♂; Bhalukpong; NCBS BH657, NCBS BH658 • 1 ♀; Sonai Rupai Wildlife Sanctuary; NCBS BH659 • 1 ♀; Arunachal Pradesh, Kamlang Wildlife Sanctuary; NCBS BH660 • 1 spec.; West Bengal, Darjeeling District; ZSI 21021.

Pareas stanleyi (Boulenger, 1914)

CHINA • holotype; N.W. Fokien; NHMUK 1946.1.20.4.

Amblycephalus tokinensis (Angel, 1920)

VIETNAM • holotype; Haut Tonkin; MNHN-RA-1908.206.